Transcriptome and proteome analysis of soleus muscle of hormone-sensitive lipase-null mice

Ola Hansson,[1,*] Morten Donsmark,[†] Charlotte Ling,[§] Pernilla Nevsten,[**] Mikael Danfelter,[*] Jesper L. Andersen,[††] Henrik Galbo,[†] and Cecilia Holm[*]

Department of Experimental Medical Science,* Lund University, Lund, Sweden; Copenhagen Muscle Research Center,† Department of Medical Physiology, The Panum Institute, University of Copenhagen, Copenhagen, Denmark; Department of Clinical Sciences,§ Lund University, Malmoe, Sweden; National Center for High-Resolution Electron Microscopy,** Lund University, Lund, Sweden; and Copenhagen Muscle Research Center,†† Department of Molecular Muscle Biology, Rigshospitalet, University of Copenhagen, Copenhagen, Denmark

Abstract **Hormone-sensitive lipase (HSL), a key enzyme in fatty acid mobilization in adipocytes, has been demonstrated also in skeletal muscle. To gain further insight into the role and importance of HSL in skeletal muscle, a transcriptome analysis of soleus muscle of HSL-null mice was performed. A total of 161 transcripts were found to be differentially expressed. Increased mRNA levels of fructose-1,6-bisphosphatase, fructose-2,6-bisphosphatase, and phosphorylase kinase γ1A suggest a higher glycogen flux in soleus muscle of HSL-null mice. An observed increase in the utilization of glycogen stores supports this finding. Moreover, an increased amount of intramyocellular lipid droplets, observed by transmission electron microscopy, suggests decreased mobilization of lipid stores in HSL-null mice. To complement the transcriptome data, protein expression analysis was performed. Five spots were found to be differentially expressed: pyruvate dehydrogenase E1α, creatine kinase (CK), ankyrin-repeat domain 2, glyceraldehyde-3-phosphate dehydrogenase, and one protein yet to be identified. The increased protein level of CK indicates creatine phosphate degradation to be of increased importance in HSL-null mice. The results of this study suggest that in the absence of HSL, a metabolic switch from reliance on lipid to carbohydrate energy substrates takes place, supporting an important role of HSL in soleus muscle lipid metabolism.**—Hansson, O., M. Donsmark, C. Ling, P. Nevsten, M. Danfelter, J. L. Andersen, H. Galbo, and C. Holm. **Transcriptome and proteome analysis of soleus muscle of hormone-sensitive lipase-null mice.** ***J. Lipid Res.*** **2005.** 46: **2614–2623.**

Supplementary key words skeletal muscle • metabolic switch • glycogen • proteomics

The two major energy substrates found in skeletal muscle, carbohydrate and fat, are stored as glycogen and triglycerides, respectively. It is well established that during high-intensity exercise, creatine phosphate degradation and glycogen breakdown are the major energy-yielding pathways. During prolonged submaximal exercise, oxidative metabolism becomes the predominant mechanism for the muscle cell to produce ATP (1). Available fuels for oxidative metabolism include muscle glycogen, blood glucose, and NEFA. The relative reliance on these substrates is mainly determined by exercise intensity and duration. NEFA could originate either from circulating lipids or through hydrolysis of intramyocellular triglyceride stores.

In the early 1960s, Randle and coworkers (2, 3) proposed a mechanism for the coordinated control of the utilization of glucose and fatty acids and also demonstrated a mechanism for the perturbation of carbohydrate metabolism by increased fat oxidation in muscle known as the glucose-fatty acid cycle or the Randle cycle. Since then, studies have shown that increased plasma NEFA availability results in a reduction in muscle carbohydrate oxidation and glycogen utilization (4, 5). Other studies have examined the effect of reduced plasma NEFA availability on carbohydrate metabolism by administration of nicotinic acid, which decreases plasma NEFA by inhibiting lipolysis in adipose tissue (6–8). These studies have shown that a reduction of plasma NEFA availability promotes an increase in carbohydrate oxidation during exercise. An increased activation of pyruvate dehydrogenase (PDH), possibly related to a decrease in the NADH/NAD^+ ratio or an epinephrine-induced increase in calcium concentration, was also demonstrated (8). It has been shown that a low-fat diet reduces intramuscular triglyceride stores and nonplasma NEFA oxidation, whereas intramuscular glycogen stores and glycogen oxidation increase during exercise (9).

Manuscript received 24 January 2005 and in revised form 7 June 2005 and in re-revised form 25 July 2005.

Published, JLR Papers in Press, September 30, 2005.
DOI 10.1194/jlr.M500028-JLR200

[1] To whom correspondence should be addressed.
e-mail: ola.hansson@med.lu.se

Hormone-sensitive lipase (HSL), a key enzyme in fatty acid mobilization in adipocytes, has been demonstrated also in skeletal muscle (10–12). Furthermore, muscle HSL has been shown to be activated by adrenaline-mediated protein kinase A phosphorylation (10) as well as by a contraction-induced mechanism, which is independent of protein kinase A (13). The expression level varies between different muscle fiber types, being higher in oxidative than in glycolytic fibers (10). To further investigate the role of HSL in skeletal muscle, we compared the mRNA and protein expression profiles in soleus muscle from our recently developed HSL-null mice and wild-type littermates using methods of quantitative analysis of the transcriptome and proteome.

MATERIALS AND METHODS

Animals

The animals used in this study had a mixed genetic background from the inbred strains C57BL/6J and SV129 (14). In the oligonucleotide microarray analysis, in the food intake measurements, and in the Western blot analysis of FAS and parvalbumin, female mice were used. For glycogen measurements, both male and female mice were used. In all other experiments, male mice were used. The rationale for using mixed genders in this study is that the aim has been to examine major changes of expression in HSL-null mice (i.e., differences that would manifest in both genders). Furthermore, in previous studies, no gender differences were observed, except for the reported male sterility (14). The mice were housed in a 12 h light/dark cycle (lights on from 7:00 AM to 7:00 PM) and had free access to normal chow diet. Food intake was measured once per week for seven animals of each genotype over a period of 29 weeks. The animals were anesthetized using midazolam 0.4 mg/mouse (Dormicum®; Hoffman-La Roche, Basel, Switzerland) in combination with fluanison 0.9 mg/mouse and fentanyl 0.02 mg/mouse (Hypnorm®; Janssen, Beerse, Belgium). In all experiments, muscles were collected in the light period, between 8 AM and 6 PM. In the transcriptome analysis, soleus muscles from both right and left hind legs of 6-month-old mice were dissected and pooled from five animals of each genotype. In the proteome analysis, soleus muscles from both right and left hind legs of 2 month old mice were dissected and pooled from six wild-type and eight HSL-null animals. All other experiments were made on individual mice of 6 to 15 months of age. The studies were approved by the local Animal Ethics Committee.

Physical activity measurements

Physical activity was measured during the dark cycle by number of photo-beam disruptions using an open field (0.4 m × 0.4 m) 16 × 16 photo-beam system (San Diego Instruments). The animals were allowed an adaptation period of 1 h before the recording started. Movements were then recorded for a period of 2 h for four individuals of each genotype. The parameters investigated were horizontal motor activity in the periphery and in the central part of the cage, vertical motor activity, grooming, and ambulatory movements.

Oligonucleotide microarray analysis

Total soleus muscle RNA was isolated as described (15) and purified using the RNeasy Mini Kit (Qiagen). RNA integrity was evaluated with agarose gel electrophoresis and with an Agilent Bioanalyzer 2100. cDNA synthesis, labeling, RNA fragmentation, hybridization, staining, scanning, and image analysis were performed at the Swegene Microarray Resource Center (http://www.swegene.org/microarray), a member of the Academic Microarray Core Laboratory Program. Briefly, cDNA was synthesized using the SuperScript Choice system (Invitrogen Life Technologies) and converted to biotin-labeled, double-stranded copy RNA (cRNA) using the Enzo RNA transcript-labeling kit recommended by Affymetrix. The cRNA was purified and fragmented at 94°C for 35 min in 40 mM Tris-acetate, pH 8.1, 100 mM KOAc, and 30 mM MgOAc. After quality verification using test arrays, the fragmented cRNA was hybridized to Mouse Genome U74A version 2 chips (MG-U74Av2) according to Affymetrix recommendations in an Affymetrix Genechip hybridization oven 640. The arrays were washed on an Affymetrix fluidics station 400 and stained with *R*-phycoerythrin streptavidin (Molecular Probes) according to the manufacturer's instructions. Visualization was performed on a Hewlett-Packard GeneArray scanner. The pooled samples were analyzed in duplicate. The data are available at the Gene Expression Omnibus website under series number GSE1772 (http://www.ncbi.nlm.nih.gov/geo/).

Data analysis

Two independent filters were applied serially to obtain a list of candidate transcripts for differential expression between the two genotypes. The first filter excluded all genes with a detection $P > 0.05$ on all four chips. Transcripts that passed this first filter were subjected to the second filter. Only transcripts with a change P value of <0.1 or >0.9 were considered as candidate transcripts for differential regulation, with a calculated 5% false-positive rate attributable to experimental variation.

Real-time quantitative PCR

Total soleus muscle RNA was isolated as described (15) and purified using the RNeasy Mini Kit (Qiagen). RNA integrity was verified with agarose gel electrophoresis. Total RNA (1 μg) was treated with DNase I (DNase I amplification grade; Invitrogen) and then reverse-transcribed using random hexamers (Amersham Biosciences) and SuperScript™ II RNaseH reverse transcriptase (Invitrogen Life Technologies) according to the manufacturer's recommendations. The mRNA levels of FAS and PDH E1α were quantified using real-time quantitative PCR performed on a LightCycler (Roche) using LightCycler FastStart DNA Master^{PLUS} SYBR Green I (Roche). 18S rRNA was used as a control to normalize gene expression. Omitting reverse transcriptase in the reactions checked the absence of contamination by genomic DNA. The efficiency of the real-time quantitative PCR of FAS and PDH E1α were calculated to 100% and 97%, for a dilution series ranging from 0.25 to 25 ng. In the experiment, 12.5 ng of reverse-transcribed sample RNA in 20 μl reaction volumes was used. The primers used were 5′-TGGTGAATTGTCTCCGAAAAGAG-3′ as forward and 5′-CACGTTCATCACGAGGTCATG-3′ as reverse primer for FAS and 5′-CCACCTCATCACTGCCTATC-3′ as forward and 5′-AGCACAACCTCCTCTTCGTC-3′ as reverse primer for PDH E1α. Each sample was analyzed in duplicate (wild-type n = 5, HSL-null n = 4). The mRNA levels of fructose-1,6-bisphosphatase, PDH kinase 4, TRAP 220, myosin heavy chain (MHC) IIb, myocyte-specific enhancer factor 2C (MEF2C), transketolase (TKT), stearoyl-CoA desaturase-1 (SCD-1), and SCD-2 were quantified using TaqMan real-time PCR with an ABI 7900 system (Applied Biosystems, Foster City, CA). Each sample was analyzed in triplicate, except for SCD-1 and SCD-2, which were analyzed in duplicate (wild-type n = 5, HSL-null n = 4), and the expression was calculated according to the standard curve method based on a two-step serial dilution with RNA content ranging from 80 to 1.25 ng. The transcript quantities were normalized to cyclophilin A. Gene-specific primer pairs and probes for fructose-1,6-bisphosphatase (Assays-on-demand, Mm00484280-

m1; Applied Biosystems), PDH kinase 4 (Mm00443325-m1), TRAP 220 (Mm00501992-m1), MHC IIb (Mm01332531-g1), MEF2C (Mm00600423-m1), TKT (Mm00447559-m1), SCD-1 (Mm00772290-m1), SCD-2 (Mm00485951-g1), and cyclophilin A (forward primer, 5′-GGGTTCCTCCTTTCACAGAATTATT-3′; reverse primer, 5′-CCGCCAGTGCCATTATGG-3′; probe, 5′-FAM-TAA-AGTCACCACCCTGGCACATGAATCCT-TAMRA-3′) were used together with 1× TaqMan® Universal PCR Master Mix (Applied Biosystems) and 20 ng of reverse-transcribed sample RNA in 10 μl reaction volumes. The expression changes were verified not only on a new set of animals but also on the same samples used in the oligonucleotide microarray analysis (data not shown).

Western blot analysis

Soleus muscles were dissected and snap-frozen in liquid nitrogen and homogenized with a glass-Teflon homogenizer in 0.25 M sucrose, 1 mM EDTA, pH 7.0, 1 mM dithiothreitol, 20 μg/ml leupeptin, 2 μg/ml antipain, and 10 μg/ml pepstatin A. The samples were sonicated briefly and centrifuged at 15,000 *g* for 15 min at 4°C. The clear supernatants were stored at −80°C in aliquots until analyzed further. Proteins (5 μg) were resolved by SDS-PAGE and electroblotted to nitrocellulose membranes. Detection of protein was accomplished using PDH E1α specific monoclonal antibodies (Molecular Probes) and rabbit anti-cyclophilin B polyclonal antibodies (Abcam) as a loading control. For the detection of FAS protein, a polyclonal rabbit anti-mouse FAS antibody was used (Santa Cruz Biotechnology) and monoclonal anti-α-tubulin antibody was used as a loading control (Sigma). For the detection of parvalbumin, a polyclonal rabbit anti-rat skeletal muscle parvalbumin antibody was used (Abcam). PDH E1α Western blots were developed using ^{125}I-labeled anti-rabbit secondary antibodies on a FLA 3000 scanner (Fuji Film). Parvalbumin and FAS Western blots were developed using a charge-coupled device camera (LAS 1000; Fuji Film).

Two-dimensional gel electrophoresis

Soleus muscles were dissected and snap-frozen in liquid nitrogen and crushed to a fine powder under liquid nitrogen using a mortar and pestle. The powder was solubilized in a sample solution containing 9.5 M urea, 1% (w/v) dithiothreitol, 2% (w/v) CHAPS, and 0.8% (v/v) carrier-ampholyte pH 3–10, shaken for 1 h, and centrifuged at 40,000 *g* for 45 min. The clear supernatant was recovered, and total protein was measured with the 2-D Quant kit (Amersham Biosciences). Samples were stored in aliquots at −80°C until analysis. Immobiline DryStrips (17 cm, pH 3–10 nonlinear; Bio-Rad) were used for isoelectric focusing (IEF). Before IEF, each strip was rehydrated in 300 μl of rehydration solution containing 50 μg of solubilized soleus muscle protein for analytical gels. The rehydration consisted of 9.5 M urea, 1% (w/v) dithiothreitol, 2% (w/v) CHAPS, and 1% (v/v) IPG buffer 3-10. Strips were allowed to rehydrate overnight under a layer of mineral oil at 20°C and 50 V in a Protean IEF cell (Bio-Rad). Focusing was carried out at 250 V for 1 h, 500 V for 1 h, 1,000 V for 1 h, 1,000 to 8,000 V over 30 min, and then 8,000 V for 30 kVh to reach steady state. After IEF, the strips were equilibrated for 15 min in a solution containing 6 M urea, 30% (w/v) glycerol, 2% (w/v) SDS, 50 mM Tris-HCl, pH 8.8, 65 mM dithiothreitol, and a trace of bromophenol blue. In a second step, the strips were equilibrated for an additional 15 min in the same solution except that dithiothreitol was replaced by 260 mM iodoacetamide. All second-dimension runs were performed in the Ettan Daltsix electrophoresis system (Amersham Biosciences) according to the manufacturer's recommendations (12.5% T, 0.8% C, continuous). All strips were sealed at the top of the second-dimension gels with 0.5% agarose and run overnight until the tracking dye had reached the anodic end.

Staining and image acquisition

Analytical gels were silver-stained according to Blum, Beier, and Gross (16) and allowed to develop for 2.5 min. Gels were scanned using an Expression 1680 Pro scanner (Epson). The two-dimensional PAGE image computer analysis was carried out using the Phoretix 2D version 2002.01 software package (Nonlinear Dynamics). Spots were detected, quantified, and matched automatically and then controlled manually. Background subtraction was performed by the nonspot method. Differential analysis was performed and spots that were overexpressed and underexpressed by >2-fold were analyzed further. Relative volumes were calculated with normalization to total volume of spots present on the individual gel to correct for staining and loading differences. Only spots that were present on all gels were used for normalization.

Identification and characterization of proteins in spots

Protein spots were excised using pipette tips and transferred to original Eppendorf tubes. The gel pieces were washed using Milli-Q water and destained with 40% (v/v) acetonitrile (Scharlau) and 25 mM NH_4HCO_3 (Sigma), pH 7.8. Subsequently, a SpeedVac concentrator was used to dry the gel pieces before the proteins were reduced with 10 mM dithiothreitol (Sigma) in 25 mM NH_4HCO_3, pH 7.8, at 56°C for 30 min. Superfluous solution was removed before the proteins were alkylated using 55 mM iodoacetamide (Sigma) in 25 mM NH_4HCO_3, pH 7.8, in complete darkness at room temperature for 30 min. The gel pieces were then washed with 40% acetonitrile and 25 mM NH_4HCO_3, pH 7.8, and dried in a SpeedVac. Digestion proceeded overnight at 37°C with 3–5 μl of trypsin (Promega), 20 μg/ml, in 25 mM NH_4HCO_3, pH 7.8. An additional 10–20 μl of buffer was applied to the gel pieces depending on their size. The digestion was terminated by the addition of 5–10 μl of 2% trifluoroacetic acid. The sample solution was purified and concentrated using reversed-phase tips, either commercially available $ZipTip_{\mu\text{-}C18}$ (Millipore) according to the manufacturer's instructions or homemade Stop and Go extraction tips (17). Similar solutions were used for StageTips as for ZipTips. Anchorchip™ target plates (Bruker Daltonik GmbH, Bremen, Germany) were prepared with 1 μl (3 mg/ml) 2,5-dihydroxybenzoic acid (DHB; Bruker) in 50% acetonitrile and 0.1% trifluoroacetic acid. The retained peptides were eluted onto the dried DHB spots using 50% acetonitrile and 0.1% trifluoroacetic acid. Matrix and sample applications were performed according to the instructions in the AnchorChip manual provided by Bruker.

Mass spectrometry

Mass spectrometric data were collected using a Bruker Scout 384 Reflex III matrix-assisted laser desorption/ionization time-of-flight mass spectrometer (MALDI TOF MS) in reflex mode with delayed extraction and an acceleration voltage of 25 kV. To improve the signal-to-noise ratio, 50–100 spectra were summarized. Trypsin autolysis peaks at 842.5100 *m/z* and 2211.1046 *m/z* were used for internal calibration. Spectra were annotated, and the peptide mass lists were exported to the ProFound™ peptide mass fingerprint program at The Rockefeller University for protein identification (http://prowl.rockefeller.edu/profound_bin/WebProFound.exe). Generally, the National Center for Biotechnology Information database was used, one missed cleavage was allowed, all cysteines were considered to be alkylated, methionines were allowed to be oxidized, and the mass tolerance was set to 0.1 Da.

Glycogen utilization

The mice were anesthetized by subcutaneous injection of fentanyl/fluanisone (Hypnorm-Dormicum 100 liters/10 g body weight). The soleus muscles were gently dissected free with intact tendons.

Ligatures were placed around the tendons. The muscles were then transferred to test tubes containing Krebs-Henseleit buffer supplemented with 8 mM glucose (Sigma, G-7528), 1 mM pyruvate (Sigma, P-8574), 1 mM palmitic acid (Sigma, P-5585), and 4% BSA (Sigma, A-6003) (PI buffer) and gassed with 95% O_2 and 5% CO_2. Afterward, soleus muscles still kept in PI buffer were gently dissected free of adipocytes with a microscope. To stabilize the muscles, they were incubated for 2 h in PI buffer and then either frozen in liquid nitrogen or incubated for an additional 8 h before being frozen.

Glycogen measurements

Approximately 5 mg of soleus muscle was homogenized in methanol-chloroform (1:1, v/v) and kept at room temperature for 30 min. Next, the homogenate was centrifuged at 2,600 *g* for 20 min at 4°C. The supernatant was removed and the pellet was resuspended in 2 ml of methanol-chloroform and centrifuged as stated above. The supernatant was removed and the pellet was used for glycogen measurements as described previously (10).

Transmission electron microscopy

Electron microscopy was chosen to estimate the amount of intramuscular lipid depots because of the well-known technical difficulty associated with biochemical measurement of this energy substrate depot in skeletal muscle samples (18). Soleus muscles were dissected and fixed in 3% glutaraldehyde in PBS buffer overnight. After washing in cacodylate buffer (0.2 M), postfixation was performed in osmium tetroxide (1% in 0.1 M cacodylate buffer) on ice, followed by washing three times in cacodylate buffer (0.1 M) and two times in Milli-Q water. En-bloc staining was performed on ice with 1% uranyl acetate during 1 h, followed by washing with Milli-Q water for 1 h. Chemical dehydration was performed in 2,2-dimethoxypropane for 30 min, followed by rinsing with acetone twice for 15 min. Spurr's resin was infiltrated gradually and then cured at 70°C for 16 h. Thin sections (50 nm) were cut with a diamond knife and an ultramicrotome (Leica UCT) and collected on glow-discharged, carbon-coated, Formvar-filmed copper grids. The sections were then observed in a Philips CM 120 Biotwin instrument at 120 kV.

MHC analysis

MHC analysis was performed using SDS-PAGE according to Andersen and Aagaard (19). Briefly, soleus muscles were homogenized in lysis buffer and heated for 3 min at 90°C; 5–20 μl of the myosin-containing samples was loaded on a SDS-PAGE gel containing 6% polyacrylamide and 30% glycerol. Gels were run at 70 V for 42 h at 4°C. Subsequently, the gels were stained with Coomassie blue, and MHC isoform content was determined with a densitometric system (Cream 1D; KemEnTec Aps, Copenhagen, Denmark).

Statistics

Data are expressed as means ± SEM, and differences were analyzed using the nonparametric Mann-Whitney *U*-test. $P < 0.05$ was considered significant.

RESULTS

Food intake and physical activity measurements

No significant difference was found in food intake between HSL-null mice and wild-type littermates, measured over a period of 29 weeks (HSL-null, 78.2 kcal/mouse/week; wild type, 79.9 kcal/mouse/week). Different parameters of physical activity were assessed by number of photobeam breaks over a period of 2 h in the dark. No significant differences were found in the investigated parameters between HSL-null mice and wild-type littermates (data not shown; n = 4).

Oligonucleotide microarray analysis

Affymetrix oligonucleotide microarrays (MG-U74Av2) were used to screen for candidate transcripts differentially regulated in soleus muscle from HSL-null mice compared with wild-type littermates. A first filter was applied to exclude transcripts with low signals (detection $P < 0.05$). To be able to estimate experimental variation, two comparison setups were used: one true comparison and one to estimate experimental error. The number of changed transcripts (i.e., the sum of upregulated and downregulated transcripts) in the two setups is plotted against change *P* value in **Fig. 1**. The difference in the number of changed transcripts between the two setups corresponds to transcriptional differences that cannot be attributed to experimental variation. Based on these comparisons, the change *P* value was set to <0.1 or >0.9, corresponding to a false-positive rate of ~5% attributable to experimental variation. Only experimental variation could be assessed because pooled material was used.

Annotated transcripts found to be differentially expressed in HSL-null mice compared with wild-type littermates are presented in **Table 1**. Of the ~12,000 genes and expressed sequence tags represented on the MG-U74Av2 chip, 161 transcripts passed the two exclusion filters. Of these 161 candidates, the expression levels of 84 transcripts were found to be increased and 77 were found to be decreased. For some genes, more than one value for the expression change is given. These genes were represented more than once on the MG-U74Av2 microarray. In all cases examined, comparable expression changes were obtained for

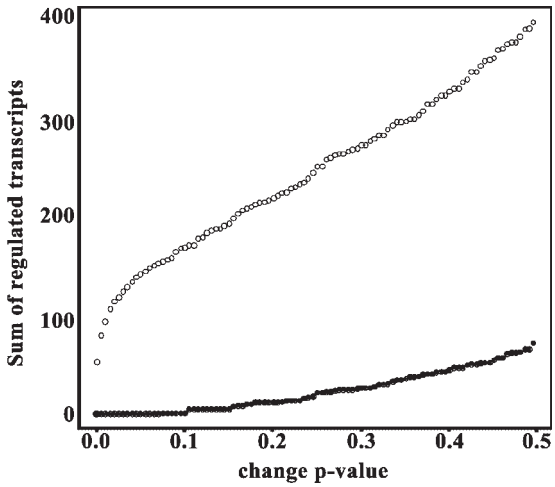

Fig. 1. Number of differentially expressed transcripts. The sum of regulated transcripts (*y* axis) is plotted against change *P* value (*x* axis). Open circles represent the true comparison, and closed circles represent the estimation of experimental variation. The difference in the number of changed transcripts between the two setups corresponds to transcriptional differences that cannot be attributed to experimental variation.

TABLE 1. Genes differentially expressed in hormone-sensitive lipase-null mice versus wild-type mice

Accession Number	Gene/Protein Name	Symbol	Expression Change
Carbohydrate metabolism			
J03293	Phosphorylase kinase γ1, skeletal muscle isoform	PHKG1	1.37
D42083	Fructose-1,6-bisphosphatase	FBP2	1.34 (1.69)[a]
X98848	Fructose-2,6-bisphosphatase	PFKFB1	1.27
Lipid metabolism			
U89906	α-Methylacyl-CoA racemase	AMACR	1.23
X95279	Thyroid hormone-responsive SPOT14	THRSP	0.83
M26270	Stearoyl-CoA desaturase 2	SCD2	0.76 (0.69)[a]
U05809	Transketolase	TKT	0.71 (0.89)[a]
M21285	Stearoyl-CoA desaturase 1	SCD1	0.62 (0.65)[a]
M21285	Stearoyl-CoA desaturase 1	SCD1	0.55 (0.65)[a]
X13135	Fatty acid synthase	FASN	0.48 (0.52)[a]
Other metabolism			
AF058955	Succinyl-CoA synthetase	SUCLA2	1.30
AF058955	Succinyl-CoA synthetase	SUCLA2	1.25
U20611	Peroxiredoxin	PRDX2	1.23
M88694	Thioether *S*-methyltransferase	TEMT	0.60
AI854020	Cysteine dioxygenase T1	CDO1	0.41
Transcription regulation			
AF000294	Peroxisome proliferator-activated receptor binding protein	PPARBP	1.93 (2.95)[a]
AA002843	Lymphoblastomic leukemia	LYL1	1.65
M28845	Early growth response	EGR1	1.65
X16995	Early response protein NAK1	NR4A1	1.39
AF022992	Period homolog 1 (*Drosophila*)	PER1	1.39
U41465	Zinc finger protein 51	BCL6	1.30
Z16406	Mesenchyme homeobox 2	MEOX2	1.30
L13171	Myocyte-specific enhancer factor 2C	MEF2C	1.25 (1.21)[a]
Y15163	Cbp/p300-interacting transactivator	CITED2	1.21
D88791	Cysteine-rich protein 3	CSRP3	0.86
L35032	Sex-determining region Y-box 18	SOX18	0.81
U19799	Nuclear factor κB inhibitor β	NFKBIB	0.80
AF077861	Inhibitor of DNA binding 2	IDB2	0.78
Z47088	RNA polymerase II elongation factor	ELL	0.78
U19118	Activating transcription factor 3	ATF3	0.78
AF015260	Mothers against decapentaplegic homolog 7	MADH7	0.78
AF041847	Cytokine-inducible nuclear protein	CARP	0.78
AB014494	Aryl hydrocarbon receptor nuclear translocator-like	ARNTL	0.72
Structural			
AJ223361	Myosin heavy chain IIb	MYH4	6.73 (3.38)[a]
AF093775	Actinin, α3	ACTN3	2.30
X58251	Collagen, type I, α1	COL1A1	1.32
D13664	Periostin, osteoblast-specific factor 2	OSF2	1.30
X69902	Integrin, α6	INTGA6	1.27
X94998	Fibromodulin	FMOD	1.27
AA763466	Collagen, type I, α2	COL1A2	1.27
M74753	Myosin heavy chain polypeptide 3, embryonic	MYH3	0.80
M18775	Microtubule-associated protein τ	MAPT	0.78
D89571	Amphiglycan	SDC4	0.77
M90365	Junction plakoglobin (desmoplakin III)	JUP	0.77
Signal transduction/signaling			
AF058799	14-3-3γ, KCIP-1	YWHAG	1.46
U83509	Angiopoietin 1	ANGPT1	1.44
X76850	Mitogen-activated protein kinase-activated protein kinase 2	MAPKAPK2	1.44
V00727	Proto-oncogene protein c-fos	FOS	1.39
AB016080	Kinase-interacting protein 2	KIP2	1.37
AJ250489	Calcitonin receptor-like receptor activity-modifying p1	RAMP1	1.34
U18996	Growth factor receptor-bound protein 10	GRB10	1.32
M57647	Mast cell growth factor	KITLG	1.30
D10712	Neural precursor cell-expressed, developmentally down-regulated gene 1	NEDD1	1.25
U67188	Regulator of G-protein signaling 5	RGS5	1.21
Y17808	Protein tyrosine kinase 9-like (A6-related protein)	PTK9L	1.19
AF033566	Protein tyrosine kinase STY, CDC-like kinase	CLK1	1.19
Z38015	Myotonic dystrophy protein kinase	DMPK	0.87
AF084466	GTP binding protein	RRAD	0.84
D45859	Protein phosphatase 1B (formerly 2C)	PPM1B	0.81
AJ010045	Neuroepithelial cell-transforming gene 1	NET1	0.81
AF067806	Phosphodiesterase 8A	PDE8A	0.80
D13695	Interleukin 1 receptor-like 1	IL1RL1	0.71
U16959	FK506 binding protein 5	FKBP5	0.69
U35233	Endothelin-1	EDN1	0.68

TABLE 1. (*Continued*)

Accession Number	Gene/Protein Name	Symbol	Expression Change
Membrane transport			
U48398	Aquaporin 4	AQP4	1.44
U88623	Aquaporin 4	AQP4	1.41
AJ006036	Solute carrier family 22	SLC22A2	1.41
M63801	Connexin 43	GJA1	1.37
X96737	VAMP-7	SYBL1	1.34
M25944	Carbonic anhydrase II	CA2	1.27
L02914	Aquaporin 1	AQP1	1.25
Others			
X59382	Parvalbumin	PVALB	1.90 (1.63)[b]
X59382	Parvalbumin	PVALB	1.74 (1.63)[b]
X86000	α-2,8-Sialyltransferase 8D	SIAT8D	1.49
AJ007749	Caspase 8	CASP8	1.30
X13605	Histone H3.3	H3F3B	0.87
X52643	Major histocompatibility complex, class II, DQ α1	HLA-DQA1	0.84
V00835	Metallothionein 1A	MT1A	0.83
X95280	Putative lymphocyte G0/G1 switch protein 2	GOS2	0.83
AB014721	Squamous cell carcinoma antigen recognized by T-cells	SART1	0.83
Y15003	Sialyltransferase 9	SIAT9	0.81
X00496	HLA class II histocompatibility antigen, γ chain	CD74	0.78
U49430	Ceruloplasmin	CP	0.76
M12571	Heat shock 70 kDa protein 1	HSPA1A	0.76
U79523	Peptidyl-glycine α-amidating monooxygenase	PAM	0.73

[a] Genes analyzed with real-time quantitative PCR; values in parentheses.
[b] The parvalbumin protein level was confirmed using Western blot analysis; values in parentheses.

these transcripts. Annotated genes were divided into six functional groups (Table 1). Among the 15 genes grouped under metabolism, two genes are involved in the same step (second bypass) in gluconeogenesis, fructose-1,6-bisphosphatase and fructose-2,6-bisphosphatase, both having increased expression levels (1.34 and 1.27, respectively) in the HSL-null mice. The changed mRNA level of fructose-1,6-bisphosphatase was confirmed (1.69) using real-time quantitative PCR (Table 1, footnote a). Phosphorylase kinase γ1 also showed an increased (1.37) mRNA level. Phosphorylase kinase regulates the activity of glycogen phosphorylase, which catalyzes the breakdown of glycogen to glucose-1-phosphate. A majority of metabolic enzymes with decreased expression levels in HSL-null mice are involved in fatty acid biosynthesis, including FAS (0.48) and SCD-1 and SCD-2 (0.62, 0.55, and 0.76, respectively). SCDs are the rate-limiting enzymes in the biosynthesis of monounsaturated fatty acids. The changed mRNA levels of FAS, SCD-1, and SCD-2 were confirmed (0.52, 0.65, and 0.69, respectively) using real-time quantitative PCR (Table 1, footnote a). A comparable reduction of the protein level of FAS (0.41; $P < 0.05$) was also found using Western blot analysis (**Fig. 2**). TKT was found to have a decreased expression level (0.71). TKT is part of the pentose phosphate pathway, in which NADPH is generated, providing reducing power for fatty acid and sterol synthesis. The changed mRNA level of TKT was confirmed (0.89) using real-time quantitative PCR (Table 1, footnote a). One enzyme in the citric acid cycle, succinyl-CoA synthetase, showed increased expression (1.25 and 1.30).

Alterations in mRNA expression levels were also found for 16 genes involved in transcription. The largest difference found in this group was an increase (1.93) of peroxisome proliferator-activated receptor binding protein, also known as TRAP 220, a factor implicated in differentiation. Other changed mRNAs included myocyte-specific enhancer factor 2C (MEF2C) and cysteine-rich protein 3 (CRP3) (1.25 and 0.86, respectively), both of which are transcription factors involved in muscle differentiation and fiber type development. The changed mRNA levels of TRAP 220 and MEF2C were confirmed (2.95 and 1.21, respectively) using real-time quantitative PCR (Table 1, footnote a). The largest change of all of the transcripts was found to be in MHC IIb, with an increased expression of >6-fold (6.73). This protein is part of the contractile machinery of fast-twitch glycolytic muscle fibers. The changed mRNA level of MHC IIb was confirmed (3.38) using real-time quan-

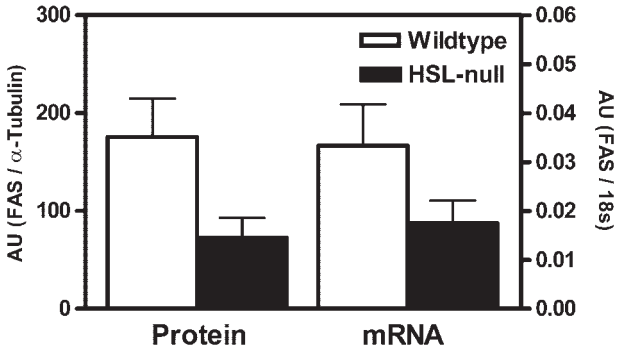

Fig. 2. FAS mRNA and protein levels in hormone-sensitive lipase (HSL)-null mice compared with wild-type littermates. The mRNA levels of 6-month-old male mice were measured using real-time quantitative PCR, and the protein levels of 10 month old female mice were measured using Western blotting. AU, arbitrary units. Values are given as means ± SEM; protein n = 3 in each group analyzed in duplicate, and mRNA n = 5–6 in each group analyzed in triplicate.

titative PCR (Table 1, footnote a). In connection with this finding, an increased expression level (1.90 and 1.74) of parvalbumin was found. Parvalbumin is also expressed in fast-twitch glycolytic type IIb muscle fibers and is believed to be involved in muscle relaxation. The increased mRNA expression of parvalbumin was confirmed at the protein level (1.63) using Western blot analysis.

Protein expression profiling

Ten analytical gels, six corresponding to the wild-type pool and four to the HSL-null pool, were run and silver-stained. On average, 1,500 spots were detected on each gel. After applying a filter to exclude weak spots, ~1,000 spots remained. These spots were matched to a reference gel, and a set of average gels was made. For a spot to be included on an average gel, it had to be present on at least five of the six gels corresponding to the wild-type samples or on three of the four gels corresponding to the null samples. No spots were detected exclusively in either genotype. Fourteen spots were found to be >2-fold upregulated and 38 spots were found to be >2-fold downregulated on the average gel representing the null samples compared with the average gel representing the wild-type samples. Spots changed significantly are presented in **Fig. 3**. When attempting to identify the candidates for differential expression, spots located in the surrounding gel area were also identified. In the case of GAPDH, several spots surrounding the regulated one were identified as arising from the same protein, indicating posttranslational modification events. The changed form was found to be downregulated 52% ($P < 0.001$). GAPDH is an enzyme in the glycolysis pathway. PDH, another enzyme involved in carbohydrate metabolism, was found to be upregulated 2.0-fold ($P < 0.05$). The pyruvate dehydrogenase complex (PDC) consists of three enzymes, E1, E2, and E3. The complex catalyzes the oxidative decarboxylation of pyruvate to acetyl-CoA, feeding the citric acid cycle with carbons. The subunit identified in this screen was the E1α. Western blot analysis was performed with antibodies raised against PDH E1α. Furthermore, real-time quantitative PCR was used to investigate changes in the mRNA level of the enzyme. However, no significant changes in either protein or mRNA levels were observed (**Fig. 4**). The reason for this could be that a phosphorylation/dephosphorylation event of the PDC led to a shift in the isoelectric point of the E1α subunit, without changing the expression level of the protein. This shift in isoelectric point would be detected with two-dimensional gel electrophoresis, but not with PCR or one-dimensional Western blot analysis. In an attempt to further investigate this possible phosphorylation event, the mRNA level of pyruvate dehydrogenase kinase 4 (PDK4) was investigated, but no significant difference was observed between HSL-null mice and wild-type littermates (1.38 ± 0.21 and 1.06 ± 0.20, respectively; $P > 0.05$, n = 4–5). Ankyrin domain 2 (Ankr D2) was found to be upregulated 5.2-fold ($P < 0.001$). Ankr D2 has been reported to be involved in the hypertrophy of skeletal muscle (20). Therefore, the wet weight of excised soleus muscles was measured. However, no significant difference was observed between wild-type and HSL-null mice (data not shown). Creatine kinase (CK) was found to be upregulated 2.9-fold ($P < 0.001$) in soleus muscle from HSL-null mice compared with wild-type littermates. Spot 212 was found to be downregulated 65% ($P < 0.001$). Attempts to identify this protein with MALDI TOF MS failed.

Energy substrate utilization

Based on the screens performed at the mRNA and protein levels, a hypothesis was generated stating that the absence of HSL leads to an impaired ability of the myocyte to utilize the intracellularly stored triglycerides, which in turn results in an increased reliance on carbohydrates as energy substrate. To test this hypothesis, the glycogen content of soleus muscle was measured. Furthermore, to in-

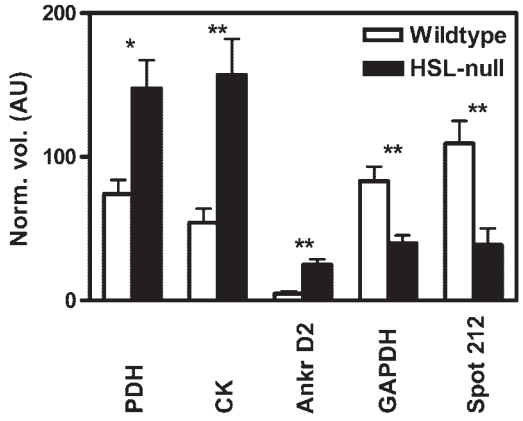

Fig. 3. Proteins differentially regulated in HSL-null mice compared with wild-type littermates. Data were generated from pooled material corresponding to six wild-type and eight HSL-null 2-month-old male mice and are expressed in arbitrary units (AU) normalized to total volume of spots. Ten analytical gels, six corresponding to the wild-type pool and four to the HSL-null pool, were analyzed. Ankr D2, ankyrin domain 2; CK, creatine kinase; PDH, pyruvate dehydrogenase. Values are given as means ± SEM. * $P < 0.05$, ** $P < 0.001$ analyzed with the Mann-Whitney *U*-test.

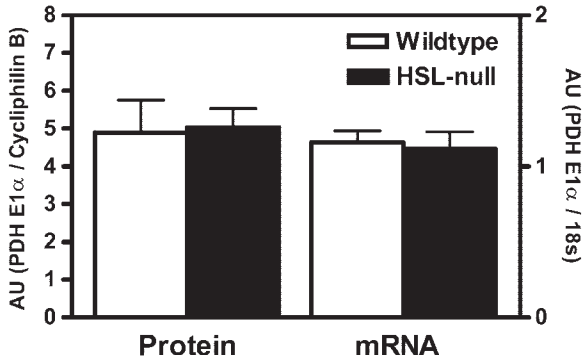

Fig. 4. PDH E1α mRNA and protein levels in HSL-null mice compared with wild-type littermates. The mRNA levels of 6-month-old male mice were measured using real-time quantitative PCR, and the protein levels of 2-month-old male mice were measured using Western blotting. AU, arbitrary units. Values are given as means ± SEM; protein n = 3 in each group analyzed in duplicate, and mRNA n = 5–6 in each group analyzed in triplicate.

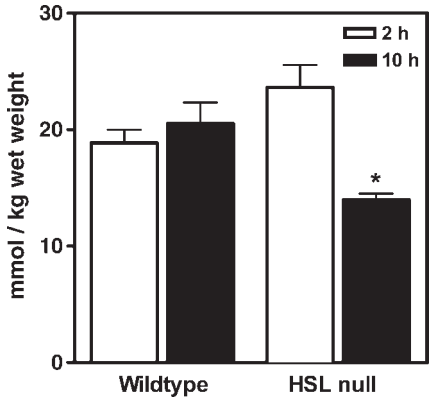

Fig. 5. Glycogen concentrations after 2 and 10 h of ex vivo incubation of soleus muscle from 6–12-month-old HSL-null and wild-type mice. A 40% reduction of total glycogen depots in HSL-null mice after 10 h of incubation compared with 2 h of incubation was observed. Values are given as means ± SEM; n = 5 for 2 h and n = 4 for 10 h in each group. * $P < 0.05$ analyzed with the Mann-Whitney *U*-test.

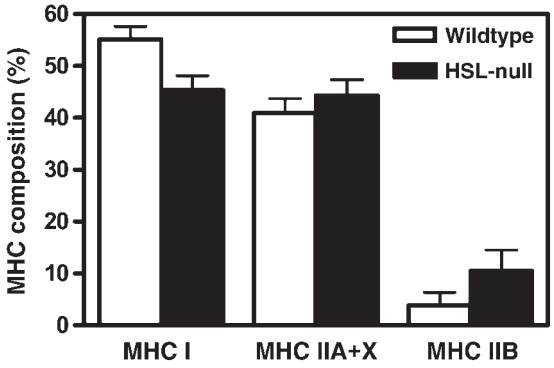

Fig. 7. Relative distribution of myosin heavy chain (MHC) isoforms in soleus muscle from 9–15 month old male mice. Values are given as means ± SEM; wild type n = 5 and HSL-null n = 7.

vestigate the utilization of the stored glycogen, excised soleus muscles were incubated ex vivo for 2 and 10 h. Significantly higher glycogen stores in soleus muscle from HSL-null mice compared with wild-type littermates have been observed in a parallel study (M. Donsmark et al., unpublished data), and a tendency in this direction was also observed in this study (**Fig. 5**), although it did not attain statistical significance because of the limited number of animals. Regarding glycogen utilization, no significant difference in glycogen stores was observed in soleus muscle from wild-type mice between the two time points, whereas in soleus muscle from HSL-null mice, a 40% ($P < 0.05$) reduction was observed (Fig. 5). Moreover, an increased amount of intramyocellular lipid droplets observed by transmission electron microscopy suggests decreased mobilization of intramuscular lipid depots in soleus muscle from HSL-null mice (**Fig. 6**).

MHC analysis

The relative distribution of MHC isoforms in soleus muscle from 9–15 month old male mice was analyzed using SDS-PAGE. A tendency toward a decreased amount of MHC I and an increased amount of MHC IIb was observed in soleus muscle from HSL-null mice compared with wild-type littermates (**Fig. 7**).

DISCUSSION

Using the methods of transcriptome and proteome analysis, we have identified a number of differentially regulated genes and proteins in soleus muscle of HSL-null mice. Changes at the mRNA level, with increased levels of enzymes involved in carbohydrate metabolism and decreased levels of enzymes involved in fatty acid biosynthesis, were observed. This, together with the observed shift in the isoelectric point of PDH E1α in the proteome screen, generated the hypothesis that in the absence of HSL a metabolic switch occurs in soleus muscle, with an increased reliance on carbohydrates and a decreased reliance on lipids as energy substrates. This, in turn, suggests that HSL plays an important role in soleus muscle lipid metabolism by mobilizing fatty acids from intracellular triglyceride stores and, furthermore, that there is little redundancy regarding this role of HSL. Thus, adipose triglyceride lipase, recently reported to be expressed in white adipose tissue as well as in skeletal muscle (21), appears not to compensate for HSL in this role. Another finding in support of an important role for HSL in soleus muscle is the increased

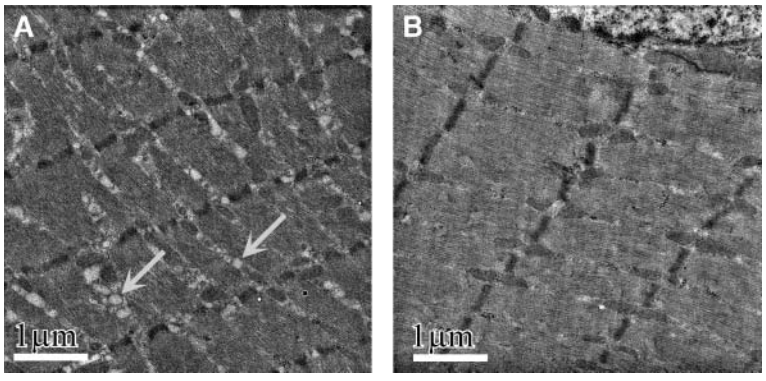

Fig. 6. Representative transmission electron microscopic images of Spurr-embedded soleus muscle from HSL-null mice (A) and wild-type littermates (B). The images were chosen from a set of ~300 recorded with a systematic random technique of 6 month old male mice, three individuals from each genotype. Examples of large lipid droplets are indicated with arrows.

amount of lipid droplets found with transmission electron microscopy. The metabolic switch hypothesis is further supported by the finding of increased glycogen utilization, shown here as decreased glycogen stores after 10 h of ex vivo incubation of excised soleus muscle. The observed increase in CK protein expression level suggests that another energy-yielding pathway (i.e., creatine phosphate degradation) has increased importance in the soleus muscle of HSL-null mice.

A key enzyme in the regulation of metabolism is the PDC. PDH E1α can be phosphorylated by PDKs, leading to an inactivation of PDC. PDK4 has been shown to be upregulated in slow-twitch muscle of rats after prolonged starvation (22) and after high-fat feeding (23), possibly providing a link between fatty acid availability and carbohydrate metabolism. In this study, the mRNA level of PDK4 was investigated, but no significant change in the expression level was observed in HSL-null mice compared with wild-type littermates. There are currently four known PDK isoforms, of which three have been shown to be expressed in skeletal muscle (i.e., PDK1, PDK2, and PDK4). Analysis of the relative expression levels in different muscle types has shown higher expression levels of PDK2 and PDK4 in oxidative muscles compared with glycolytic muscles, whereas PDK1 levels are similar (24). Two pyruvate dehydrogenase phosphatase (PDP) isoforms are known to be expressed in mammalian tissues. In skeletal muscle, PDP1 is the dominant isoform (25). The observed shift in isoelectric point of PDH E1α could be explained by changed activity of any of the kinases or phosphatases present in skeletal muscle known to influence the phosphorylation state of PDH E1α.

Based on the suggested increased reliance on carbohydrate metabolism, together with the increased mRNA expression level of MHC IIb and the increased protein levels of parvalbumin and CK, one could speculate that a fiber type transformation has occurred in soleus muscle of HSL-null mice. Soleus muscle is considered to consist mainly of slow-twitch oxidative fibers; a transformation into an enrichment of fast-twitch glycolytic fibers would be in agreement with the data presented here. In support of a fiber type transformation, a number of transcription factors known to be involved in fiber type development, such as TRAP 220, MEF2C, and CRP3, were found to be differentially regulated in the transcriptome analysis. Furthermore, when the MHC isoform distribution was examined, a tendency toward a decreased amount of MHC I and an increased amount of MHC IIb protein was observed, providing further support for the hypothesis that a fiber type transformation has occurred in soleus muscle of the HSL-null mice. Interestingly, an increase in the number of type IIb muscle fibers in insulin-resistant first-degree relatives of patients with noninsulin-dependent diabetes mellitus has been observed (26).

The seemingly conflicting observations in our HSL-null mouse strain [i.e., the previously reported insulin resistance at the level of skeletal muscle (14) and the finding in this study of an increased reliance on carbohydrates as energy substrates] may be the result of two independent responses in the muscle cell. The reduced insulin-stimulated glucose uptake could be the result of a signaling defect. In an independently generated HSL-null mouse strain, diglyceride accumulation has been observed at the level of skeletal muscle (27). Diglyceride accumulation could trigger the activation of atypical protein kinase C, leading to serine/threonine phosphorylation of insulin receptor substrate 1 and thereby perturbed insulin signaling (28). When faced with an inability to mobilize the intramuscularly stored triglycerides, the cell could respond by increasing the uptake of NEFA or triacylglycerol from the circulation. LPL activity at the level of skeletal muscle has been investigated in an independently generated HSL-null mouse strain without detecting any increase in the fed state, although a significant increase was observed in the fasted state (29). Another way for the muscle cell to generate the needed energy would be to increase glycogen utilization, as reported here. An increased lactate uptake could be one source of carbons for the increased glycogen production. Fructose-1,6-bisphosphatase activity has been shown to correlate with the uptake and incorporation of lactate into glycogen (30). This enzyme was identified in the transcriptome screen to have increased mRNA expression levels in soleus muscle from HSL-null mice. The increased expression was also verified with real-time quantitative PCR.

It is possible that the observed changes in metabolism in soleus muscle of HSL-null mice may be secondary effects caused by the absence of HSL in other tissues, such as adipose tissue. A reduction in the supply of NEFA from adipose stores would limit the ability of myocytes to utilize this energy substrate, which could be the basis for the observed metabolic switch in soleus muscle. However, under resting conditions, the rate of fatty acid uptake is usually closely related to the concentration of NEFA in the plasma. In the HSL-null mouse model examined here, no changes in plasma NEFA have been observed in the fed state (14).

In this study, no correlation was observed between data generated in the transcriptome and the proteome screens. A discrepancy between the expression levels of mRNA and protein was shown previously when comparing more comprehensive transcriptome and proteome screens (31, 32). There are at least a couple of possible explanations for this. On the one hand, posttranslational events are detected using two-dimensional gel electrophoresis. On the other hand, solubilization of hydrophobic proteins, detection of low-abundance proteins, and focusing proteins with extreme isoelectric points are common problems in the separation of proteins in tissue homogenates with two-dimensional gel electrophoresis, resulting in the detection of only a fraction of the total proteome. In comparison, essentially the whole transcriptome is analyzed with oligonucleotide microarray technology.

In conclusion, the global and functional analysis of soleus muscle of HSL-null mice in this study supports an important role of HSL in soleus muscle metabolism, as the absence of HSL leads to increased glycogen utilization and increased amounts of lipid droplets, which presumably reflect a metabolic switch from lipid to carbohydrate metabolism.

The authors thank Dr. Svante Paabo and Dr. Philipp Khaitovich for assistance with the microarray data analysis, Dr. Stephanie Lucas for assistance with the SYBR Green real-time PCR experiments, Dr. Mary C. Sugden for advising us on PDH experiments, Ann-Helen Thorén for animal breeding and genotyping, and Dr. Peter Osmark for critical reading of the manuscript. Financial support was provided by the Swedish Research Council (Project 112 84 to C.H. and Project 621-2003-300 to Reine Wallenberg at the National Center for High-Resolution Electron Microscopy), the Cell Factory for Functional Genomics, a program funded by the Swedish Foundation for Strategic Research, a Center of Excellence grant from the Juvenile Diabetes Foundation, USA, the Knut and Alice Wallenberg Foundation, Sweden, the Swedish Diabetes Association, and the following foundations: Novo Nordisk, The Lundbeck Foundation, Denmark, A. Påhlsson, Salubrin/Druvan, the IngaBritt and Arne Lundberg Research Foundation, and Torsten and Ragnar Söderberg.

REFERENCES

1. Hargreaves, M. 2000. Skeletal muscle metabolism during exercise in humans. *Clin. Exp. Pharmacol. Physiol.* **27:** 225–228.
2. Randle, P. J., P. B. Garland, C. N. Hales, and E. A. Newsholme. 1963. The glucose fatty-acid cycle. Its role in insulin sensitivity and the metabolic disturbances of diabetes mellitus. *Lancet.* **1:** 785–789.
3. Randle, P. J., P. B. Garland, C. N. Hales, E. A. Newsholme, R. M. Denton, and C. I. Pogson. 1966. Interactions of metabolism and the physiological role of insulin. *Recent Prog. Horm. Res.* **22:** 1–48.
4. Dyck, D. J., S. J. Peters, P. S. Wendling, A. Chesley, E. Hultman, and L. L. Spriet. 1996. Regulation of muscle glycogen phosphorylase activity during intense aerobic cycling with elevated FFA. *Am. J. Physiol.* **270:** E116–E125.
5. Romijn, J. A., E. F. Coyle, L. S. Sidossis, X. J. Zhang, and R. R. Wolfe. 1995. Relationship between fatty acid delivery and fatty acid oxidation during strenuous exercise. *J. Appl. Physiol.* **79:** 1939–1945.
6. Galbo, H., J. J. Holst, N. J. Christensen, and J. Hilsted. 1976. Glucagon and plasma catecholamines during beta-receptor blockade in exercising man. *J. Appl. Physiol.* **40:** 855–863.
7. Howlett, K. F., L. L. Spriet, and M. Hargreaves. 2001. Carbohydrate metabolism during exercise in females: effect of reduced fat availability. *Metabolism.* **50:** 481–487.
8. Stellingwerff, T., M. J. Watt, G. J. Heigenhauser, and L. L. Spriet. 2003. Effects of reduced free fatty acid availability on skeletal muscle PDH activation during aerobic exercise. Pyruvate dehydrogenase. *Am. J. Physiol. Endocrinol. Metab.* **284:** E589–E596.
9. Coyle, E. F., A. E. Jeukendrup, M. C. Oseto, B. J. Hodgkinson, and T. W. Zderic. 2001. Low-fat diet alters intramuscular substrates and reduces lipolysis and fat oxidation during exercise. *Am. J. Physiol. Endocrinol. Metab.* **280:** E391–E398.
10. Langfort, J., T. Ploug, J. Ihlemann, M. Saldo, C. Holm, and H. Galbo. 1999. Expression of hormone-sensitive lipase and its regulation by adrenaline in skeletal muscle. *Biochem. J.* **340:** 459–465.
11. Holm, C., T. G. Kirchgessner, K. L. Svenson, G. Fredrikson, S. Nilsson, C. G. Miller, J. E. Shively, C. Heinzmann, R. S. Sparkes, T. Mohandas, et al. 1988. Hormone-sensitive lipase: sequence, expression, and chromosomal localization to 19 cent-q13.3. *Science.* **241:** 1503–1506.
12. Holm, C., P. Belfrage, and G. Fredrikson. 1987. Immunological evidence for the presence of hormone-sensitive lipase in rat tissues other than adipose tissue. *Biochem. Biophys. Res. Commun.* **148:** 99–105.
13. Langfort, J., T. Ploug, J. Ihlemann, C. Holm, and H. Galbo. 2000. Stimulation of hormone-sensitive lipase activity by contractions in rat skeletal muscle. *Biochem. J.* **351:** 207–214.
14. Mulder, H., M. Sorhede-Winzell, J. A. Contreras, M. Fex, K. Strom, T. Ploug, H. Galbo, P. Arner, C. Lundberg, F. Sundler, et al. 2003. Hormone-sensitive lipase null mice exhibit signs of impaired insulin sensitivity whereas insulin secretion is intact. *J. Biol. Chem.* **278:** 36380–36388.
15. Chomczynski, P., and N. Sacchi. 1987. Single-step method of RNA isolation by acid guanidinium thiocyanate-phenol-chloroform extraction. *Anal. Biochem.* **162:** 156–159.
16. Blum, H., H. Beier, and H. J. Gross. 1987. Improved silver staining of plant-proteins, RNA and DNA in polyacrylamide gels. *Electrophoresis.* **8:** 93–99.
17. Rappsilber, J., Y. Ishihama, and M. Mann. 2003. Stop and go extraction tips for matrix-assisted laser desorption/ionization, nanoelectrospray, and LC/MS sample pretreatment in proteomics. *Anal. Chem.* **75:** 663–670.
18. Guo, Z., P. Mishra, and S. Macura. 2001. Sampling the intramyocellular triglycerides from skeletal muscle. *J. Lipid Res.* **42:** 1041–1048.
19. Andersen, J. L., and P. Aagaard. 2000. Myosin heavy chain IIX overshoot in human skeletal muscle. *Muscle Nerve.* **23:** 1095–1104.
20. Kemp, T. J., T. J. Sadusky, F. Saltisi, N. Carey, J. Moss, S. Y. Yang, D. A. Sassoon, G. Goldspink, and G. R. Coulton. 2000. Identification of Ankrd2, a novel skeletal muscle gene coding for a stretch-responsive ankyrin-repeat protein. *Genomics.* **66:** 229–241.
21. Zimmermann, R., J. G. Strauss, G. Haemmerle, G. Schoiswohl, R. Birner-Gruenberger, M. Riederer, A. Lass, G. Neuberger, F. Eisenhaber, A. Hermetter, et al. 2004. Fat mobilization in adipose tissue is promoted by adipose triglyceride lipase. *Science.* **306:** 1383–1386.
22. Sugden, M. C., A. Kraus, R. A. Harris, and M. J. Holness. 2000. Fibre-type specific modification of the activity and regulation of skeletal muscle pyruvate dehydrogenase kinase (PDK) by prolonged starvation and refeeding is associated with targeted regulation of PDK isoenzyme 4 expression. *Biochem. J.* **346:** 651–657.
23. Holness, M. J., A. Kraus, R. A. Harris, and M. C. Sugden. 2000. Targeted upregulation of pyruvate dehydrogenase kinase (PDK)-4 in slow-twitch skeletal muscle underlies the stable modification of the regulatory characteristics of PDK induced by high-fat feeding. *Diabetes.* **49:** 775–781.
24. Peters, S. J., R. A. Harris, G. J. Heigenhauser, and L. L. Spriet. 2001. Muscle fiber type comparison of PDH kinase activity and isoform expression in fed and fasted rats. *Am. J. Physiol. Regul. Integr. Comp. Physiol.* **280:** R661–R668.
25. Huang, B., R. Gudi, P. Wu, R. A. Harris, J. Hamilton, and K. M. Popov. 1998. Isoenzymes of pyruvate dehydrogenase phosphatase. DNA-derived amino acid sequences, expression, and regulation. *J. Biol. Chem.* **273:** 17680–17688.
26. Nyholm, B., Z. Qu, A. Kaal, S. B. Pedersen, C. H. Gravholt, J. L. Andersen, B. Saltin, and O. Schmitz. 1997. Evidence of an increased number of type IIb muscle fibers in insulin-resistant first-degree relatives of patients with NIDDM. *Diabetes.* **46:** 1822–1828.
27. Haemmerle, G., R. Zimmermann, M. Hayn, C. Theussl, G. Waeg, E. Wagner, W. Sattler, T. M. Magin, E. F. Wagner, and R. Zechner. 2002. Hormone-sensitive lipase deficiency in mice causes diglyceride accumulation in adipose tissue, muscle, and testis. *J. Biol. Chem.* **277:** 4806–4815.
28. Griffin, M. E., M. J. Marcucci, G. W. Cline, K. Bell, N. Barucci, D. Lee, L. J. Goodyear, E. W. Kraegen, M. F. White, and G. I. Shulman. 1999. Free fatty acid-induced insulin resistance is associated with activation of protein kinase C theta and alterations in the insulin signaling cascade. *Diabetes.* **48:** 1270–1274.
29. Haemmerle, G., R. Zimmermann, J. G. Strauss, D. Kratky, M. Riederer, G. Knipping, and R. Zechner. 2002. Hormone-sensitive lipase deficiency in mice changes the plasma lipid profile by affecting the tissue-specific expression pattern of lipoprotein lipase in adipose tissue and muscle. *J. Biol. Chem.* **277:** 12946–12952.
30. McLane, J. A., and J. O. Holloszy. 1979. Glycogen synthesis from lactate in the three types of skeletal muscle. *J. Biol. Chem.* **254:** 6548–6553.
31. Griffin, T. J., S. P. Gygi, T. Ideker, B. Rist, J. Eng, L. Hood, and R. Aebersold. 2002. Complementary profiling of gene expression at the transcriptome and proteome levels in *Saccharomyces cerevisiae*. *Mol. Cell. Proteomics.* **1:** 323–333.
32. Chen, G., T. G. Gharib, C. C. Huang, J. M. Taylor, D. E. Misek, S. L. Kardia, T. J. Giordano, M. D. Iannettoni, M. B. Orringer, S. M. Hanash, et al. 2002. Discordant protein and mRNA expression in lung adenocarcinomas. *Mol. Cell. Proteomics.* **1:** 304–313.